



Seasonal correlations of SST, water vapor, and convective activity in tropical oceans: A new hyperspectral data set for climate model testing

Hartmut H. Aumann,¹ David T. Gregorich,¹ Steven E. Broberg,¹ and Denis A. Elliott¹

Received 22 December 2006; revised 4 April 2007; accepted 19 June 2007; published 15 August 2007.

[1] The analysis of the response of the Earth Climate System to the seasonal changes of solar forcing in the tropical oceans using four years of the Atmospheric Infrared Sounder (AIRS) and Advanced Microwave Sounding Unit (AMSU) data between 2002 and 2006 gives new insight into amplitude and phase relationships between surface and tropospheric temperatures, humidity, and convective activity. The intensity of the convective activity is measured by counting deep convective clouds. The peaks of convective activity, temperature in the mid-troposphere, and water vapor in the 0–30°N and 0–30°S tropical ocean zonal means occur about two months after solstice, all leading the peak of the sea surface temperature by several weeks. Phase is key to the evaluation of feedback. The evaluation of climate models in terms of zonal and annual means and annual mean deviations from zonal means can now be supplemented by evaluating the phase of key atmospheric and surface parameters relative to solstice. The ability of climate models to reproduce the statistical flavor of the observed amplitudes and relative phases for broad zonal means should lead to increased confidence in the realism of their water vapor and cloud feedback algorithms. AIRS and AMSU were launched into a 705 km altitude polar sun-synchronous orbit on the EOS Aqua spacecraft on May 4, 2002, and have been in routine data gathering mode since September 2002. **Citation:** Aumann, H. H., D. T. Gregorich, S. E. Broberg, and D. A. Elliott (2007), Seasonal correlations of SST, water vapor, and convective activity in tropical oceans: A new hyperspectral data set for climate model testing, *Geophys. Res. Lett.*, *34*, L15813, doi:10.1029/2006GL029191.

1. Introduction

[2] The Earth Climate System is driven by the magnitude and the variability of the power received from the Sun. The seasonal variability is dominated by the 23.5 degree tilt of the Earth polar axis. The response to the peak of the solar power near solstice is the warming of the oceans and the troposphere and associated increases in humidity and convective activity. The understanding of the correlation and phase relationships between these atmospheric parameters is important for the realistic implementation of the cloud and water vapor feedback mechanisms in climate models. However, current evaluations of climate models are in terms of zonal and annual means and anomalies [*Intergovernmental Panel on Climate Change*, 2001]. This evaluation sup-

presses seasonal variability and phase. The determination of amplitudes and phases requires global, accurate and extremely stable data for many years. The global satellite data available for reanalysis starting in 1978 were limited to the very broad sounding channels of the High Resolution Infrared Sounder (HIRS) and the Microwave Sounding Unit (MSU), both from non-maintained polar orbits. AIRS was specifically designed to support NASA's climate research program [*Chahine et al.*, 2006]. The spectrally resolved upwelling radiances measured by AIRS give direct insight into the way the Earth Climate System responds to periodic changes in forcing with changes in surface and atmospheric temperatures, water vapor distribution and clouds.

[3] AIRS is a grating array imaging spectrometer which covers the 3.7–15.4 micron spectral region with 2378 spectral channels and spectral resolution of $v/\Delta v = 1200$. Also included in the AIRS sounder system are four VIS/NIR channels [*Gautier et al.*, 2003] and AMSU. AMSU-A has 15 sounding channels between 23 and 90 GHz. AIRS and AMSU-A were launched into a 705 km altitude polar orbit on the EOS Aqua spacecraft on May 4, 2002 and have been in routine data gathering mode essentially uninterrupted since September 2002. The 1:30 PM ascending node and orbital altitude of the EOS Aqua orbit are accurately maintained to minimize confusion of diurnal variability with climate trends. Essentially global coverage is achieved twice per day. The AIRS absolute radiometric calibration accuracy, milli-Kelvin per year radiometric stability, and frequency stability at the 1 part per million level have been documented in the literature [*Aumann et al.*, 2006a; *Strow et al.*, 2006]. More than four years of hyperspectral data from AIRS constitute one of the most powerful tools currently available for climate research. AIRS, AMSU-A and the EOS Aqua spacecraft are approaching five years on orbit without signs of significant degradation, with predictions of a twelve year lifetime.

2. Approach

[4] We have used the first four years of AIRS and AMSU-A data to analyze the seasonal variability and phase relationships between the sea surface temperature (SST) and key atmospheric parameters. The phase and amplitude relationships are complex on a regional scale, but relatively simple patterns emerge from the analysis of broad zonal means. Each day AIRS generates about 3.7 million spectra. A small subset of the AIRS and AMSU data, the AIRS Climate Data Subset (ACDS), contains: (1) nominally cloud-free spectra, (2) "random" spectra, (3) all spectra from footprints identified as deep convective clouds (DCC), and (4) spectra from overpasses of fixed ground sites of potential calibration and validation interest under clear and

¹Jet Propulsion Laboratory, California Institute of Technology, Pasadena, California, USA.

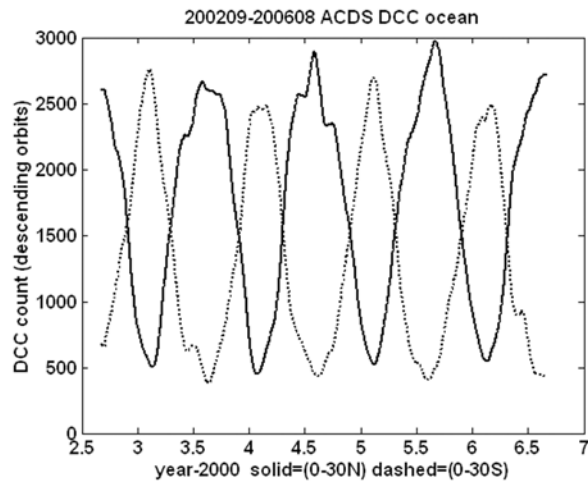


Figure 1. The deep convective cloud count illustrates the strong seasonal anti-correlation between the northern (solid) and southern (dashed) hemispheres.

cloudy conditions. The ACDS, version 4.0, in the form of one file per day, typically 300 Mbytes, is freely available via anonymous ftp at <ftp://g0dps01u.ecs.nasa.gov/AIRS/AIRX2MTL.003> from the Goddard Space Flight Center starting from August 31, 2002. Each spectrum in the ACDS is position matched to the Real Time Global SST (RTGSST), developed by the National Centers for Environmental Prediction/Marine Modeling and Analysis Branch (NCEP/MMAB) [Thiébaux *et al.*, 2003]. The cloud-free spectra are a critical component of the ACDS, since they can be used to establish absolute radiometric accuracy and stability [Aumann *et al.*, 2006a]. Since cloud-free data are not representative of state of the atmosphere relevant for climate studies, we use the random spectra in the following analysis. The random spectra are selected from footprints within 0.6 degrees of nadir using a random number generator such that their average spacing is about 150 km, irrespective of their clear or cloudy state. The approximately 2200 random spectra selected globally each day can be used to calculate statistically representative zonal means and seasonal variability about the mean, which can be compared directly to climate models. About 800 of these spectra per day fall into the ± 30 degree latitude tropical ocean zone. In addition, we use the DCC spectra to illustrate the seasonal variability of convection. The DCC are identified in the AIRS data as spectra from non-frozen ocean and land, where the brightness temperature in the 1.1 degree diameter (13.5 km at nadir) AIRS footprint is less than 210 K in the 1231 cm^{-1} window channel [Aumann *et al.*, 2006b]. Each DCC represents the extreme end of the size distribution of thunderstorms. The ratio of the DCC count to the total number of spectra per day, typically about 0.5% of all spectra tropical ocean spectra, can therefore be considered as a measure of the frequency of very strong convective activity. An equally viable indicator of convective activity would be the fraction of the oceans covered by clouds such that the cloud-top temperature in the 1231 cm^{-1} AIRS window channel is 70 K less than the surface temperature given by the RTGSST. For the tropical oceans this metric identifies typically 3% of all spectra, with virtually the same

seasonal variability as the DCC. Only the statistics of this larger data set, not the spectra, were saved in the ACDS.

3. Results

[5] The Earth Climate System responds to the seasonal change in the incident solar power with changes in the Sea Surface Temperature (SST), changes in temperature and water vapor profiles, and changes in cloud cover and associated convection. We present results for the seasonal fluctuations of SST, and geophysical parameters most easily extracted from the data: the temperature at 5 km altitude, the total water vapor, water vapor at 300 mb and the DCC count. The complete AIRS spectra include much more information, including the vertical distribution clouds and cloud composition. In the following we illustrate this seasonal variability using the DCC count.

[6] The seasonal fluctuations of the DCC count from descending (night) orbits are shown in Figure 1. The solid trace (0–30 N latitude ocean zone) and the dashed trace (0–30 S) are the result of passing the daily means through a 32 day sliding triangular-weighted filter. This suppresses the effects of the 16 day repeat cycle of the EOS Aqua orbit and regional fluctuations, creating the equivalent of monthly means. The DCC count swings seasonally from about 500 near the winter solstice to almost 3000 near summer solstice. The pattern of seasonal variation of the daily DCC count for 1:30 PM ascending orbits (daytime) is almost identical, but the count is about 10% less. Although the daily count is high, the DCC cover on average only about 0.5% of the area of the tropical oceans.

[7] The strong north/south anticorrelation seen in the DCC count is seen in the SST and throughout the troposphere in the total water column, 300 mb precipitable water, cloud height, and other parameters. This correlation is due to the relationship between the temperature and the amount of water vapor for saturated conditions, defined by the Clausius-Clapeyron equation, and was first noted by Wentz and Schabel [2000]. However, on closer inspection, there is a consistent phase shift between the SST and the water vapor. This is illustrated in Figure 2, which shows the total

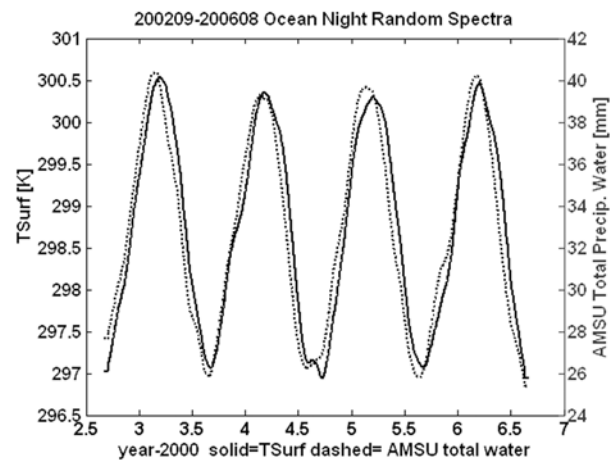


Figure 2. PW, the total precipitable water for the 0–30°S tropical oceans (dashed), overlaid on TSurf (RTGSST, solid) shows an excellent amplitude correlation, but PW leads the SST by about 2 weeks.

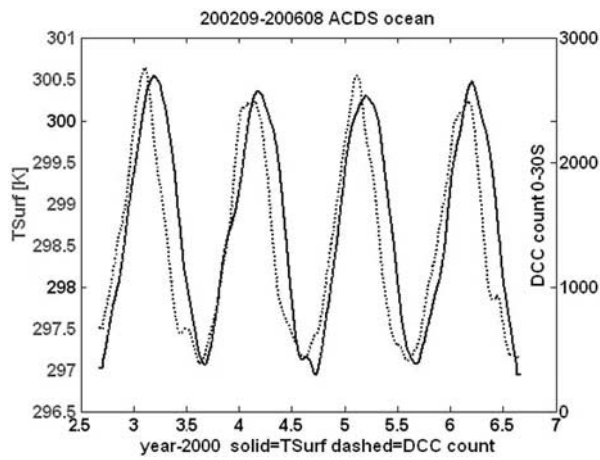


Figure 3. The DCC count for the 0–30°S tropical oceans (dashed), overlaid on the TSurf (RTGSST, solid) shows an excellent amplitude correlation, but the DCC count consistently leads the SST and drops more rapidly. By the time the SST peaks, the DCC count has already dropped about 20% below its peak value.

precipitable water, PW, in units of millimeters derived from the AMSU-A 23.8 and 31.4 GHz channels, for the 0–30°S tropical oceans as a function of time, overlaid on the RTGSST. While there is an excellent amplitude correlation, the PW leads the SST by about 2 weeks. The same phase relationship between the SST and the DCC count is shown in Figure 3. The DCC count also leads the SST by about two weeks. We intentionally used totally independent data for this illustration to eliminate the possibility of a sampling bias, correlations or phase relationships imposed by a simultaneous retrieval of surface temperature and humidity.

[8] For a quantitative analysis of peak-to-peak amplitudes and phases we assume that the daily means (not the 32 day filtered data) have a seasonal periodicity, i.e., we least-squares fit the data to a short harmonic series

$$y = a_0 + \sum (a_i \sin(2\pi i t) + b_i \cos(2\pi i t)) \quad i = 1..3.$$

The results are summarized in Table 1 for the RTGSST, the temperature at 5 km altitude (AMSU A 53.6 GHz channel), referred to as T(5 km), the total water vapor from AMSU-A, UTW300 and the DCC count in terms of the four year mean, the 32 day filtered peak-to-peak (p-p) modulation about the mean, the calendar dates of the peak and the minimum and the delay between the peak and the minimum relative to the summer and winter solstice (SS/WS). The location of the peaks and minima were rounded to the nearest 0.1 month, i.e. differences larger than 3 days are significant. UTW300 is the precipitable water in the column above 300 mb derived from the AIRS 2387 cm^{-1} and 1551 cm^{-1} channels [Aumann et al., 2005].

4. Discussion

[9] Two results emerge from our analysis of the seasonal variability of the tropical oceans.

[10] (1) The overall seasonal fluctuations were expected. The peak in the solar radiation near SS warms the atmo-

sphere and the oceans and causes a steep intensification in convective activity, resulting in a rapid increase in the tropospheric humidity, but not necessarily water vapor saturation. Our analysis of four years of AIRS data measures the seasonal variability of selected atmospheric parameters in terms of mean values, peak-to-peak amplitudes and relative phases. The overall correlation between the seasonal forcing and the response of the surface and atmospheric temperatures is no surprise. The correlation between upper-tropospheric humidity and the frequency of deep convection was first pointed out by Soden and Fu [1995], but our data show that this correlation holds for the total and 300 mb precipitable water vapor. The most interesting part of Table 1 are the two columns showing the phase lag, i.e. the number of days between the peak (peak-SS) and minimum (min-WS) of each parameter relative to the summer and the winter solstice. UTW300, PW, T(5 km) and the DCC count show a two months time lag in (peak-SS), but the SST lags 2–3 weeks behind. By the time the SST peaks, the DCC count has already dropped about 20% below its peak value. The additional delay in the SST is due to the thermal inertia of the mixed layer. There are small but consistent differences between the (peak-SS) and (peak-WS). Most notably, the UTW300 responds much quicker than the other parameters relative to the WS, likely due to cloud feedback effects. The land fraction for the tropical zone 0–30°N and 0–30°S is fairly comparable, 26% and 23%, so the differences in the phase lag between NH/SH are likely due to the near coincidence of perihelion with the SH summer solstice.

[11] (2) The seasonal pattern derived from the broad zonal means of the four years between 2002 and 2006 produces relatively stable amplitudes and phase shifts. Phase is critical to the understanding of feedback. The statistical flavor of the observed values, obviously not the exact values, should be reproduced by climate models. The seasonal modulation of the power available from the Sun can thus be used as a test of the dynamic response of climate models to external forcing. In addition to the parameters shown in Table 1, the zonal means of cloud height, cloud fraction, lapse rate, height of the tropopause, and stratospheric temperatures show similar

Table 1. Summary of the Amplitude and Phase Relationship of Northern Hemisphere and Southern Hemisphere Tropical Ocean Temperature, Total Water Vapor, 5 Km Temperature, 300 Mb Water Vapor, and DCC Count Relative to the Summer Solstice and Winter Solstice^a

| | Mean | P-P | Peak | Peak-SS | Minimum | Min-WS |
|-----------|---------|---------|---------|---------|---------|---------|
| NH | | | | | | |
| SST | 300.2 K | 2.4 K | 21 Sept | 90 days | 21 Feb | 90 days |
| T(5 km) | 258.8 K | 1.4 K | 24 Aug | 63 days | 12 Feb | 51 days |
| PW | 39.5 mm | 14.2 mm | 24 Aug | 63 days | 15 Feb | 54 days |
| UTW300 | 0.14 mm | 0.06 mm | 21 Aug | 60 days | 6 Feb | 45 days |
| DCC count | 1709 | 2274 | 24 Aug | 63 days | 12 Feb | 51 days |
| SH | | | | | | |
| SST | 298.8 K | 3.5 K | 15 Mar | 84 days | 1 Sept | 70 days |
| T(5 km) | 258.3 K | 1.6 K | 27 Feb | 68 days | 21 Aug | 60 days |
| PW | 32.6 mm | 14.5 mm | 27 Feb | 68 days | 15 Aug | 54 days |
| UTW300 | 0.11 mm | 0.07 mm | 3 Mar | 64 days | 27 Jul | 36 days |
| DCC count | 1156 | 1016 | 12 Feb | 51 days | 15 Aug | 54 days |

^aNorthern Hemisphere, NH; Southern Hemisphere, SH; tropical ocean temperature, SST; total water vapor, PW; 5 km temperature, T(5 km); 300 mb water vapor, UTW300; summer solstice, SS; winter solstice, WS.

stable seasonal behavior for the tropical oceans. A close match between observations and climate-model-derived mean, modulation and phase of key surface and atmospheric parameters for broad zonal means will serve to greatly enhance the confidence in the accuracy of the model's water vapor and cloud feedback implementation.

[12] The seasonal patterns for the tropical oceans derived from only four years of data produce fairly stable results, since the 2002–2006 period was very stable. Potential effects of interannual variability, including El Niño events, may make a longer time series desirable for the evaluation of climate models. With the exception of UTW300, the results discussed from four years of data can be derived for more than one decade from already available data: The RTGSST has been available since the year 2000. The total precipitable water column can be derived from AMSU, SSM/I or the TMI as far back as 1997 [Wentz *et al.*, 2001]. The derivation of a consistent DCC count or an equivalent measure of convective activity from archival HIRS and AVHRR data as far back as 1978 is possible, but the different ascending nodes of different spacecraft orbits and the lack of orbit maintenance require corrections for the diurnal cycle.

5. Conclusions

[13] Spectrally resolved upwelling infrared radiances give direct insight into the way the Earth Climate System responds to periodic changes in solar incident flux with changes in surface and atmospheric temperatures, water vapor distribution and clouds. We use the AIRS Climate Data Subset derived from four years of Atmospheric Infrared Sounder and AMSU-A data to evaluate the response of the Earth Climate System to seasonal changes in the tropical oceans. The peaks of convective activity, temperature in the mid-troposphere, and water vapor in the 0–30 N and 0–30 S zonal means occur about two months after solstice, all leading the peak of the sea surface temperature by several weeks. The response for the four years of data was stable and seasonally repetitive. The seasonal modulation of the solar radiative forcing can be used to compare the observed response of the Earth Climate System to the response of climate models in phase and amplitude. The ability of climate models to reproduce the statistical flavor of the observations for broad zonal means should lead to

increased confidence in their water vapor and cloud feedback algorithms.

[14] **Acknowledgments.** The AIRS spectrometer was the fruit of a relentless effort led by Moustafa Chahine, supported by a large team and funded by NASA HQ under program scientist Ramesh Kakar. The impressive long term radiometric and spectral stability of the AIRS instrument is a tribute to the instrument design concept developed by the JPL team under Fred O'Callaghan, and the careful attention to details of the design by the BAE team under Jerry Bates and Paul Morse. The research described in this paper was carried out at the Jet Propulsion Laboratory, California Institute of Technology, under a contract with the National Aeronautics and Space Administration.

References

- Aumann, H. H., D. Gregorich, and E. Dobkowski (2005), Atmospheric Infrared Sounder data for the evaluation of upper tropospheric water maps for short term weather forecasting, paper presented at Photonics Conference, SPIE, San Diego, Calif., 31 July–4 Aug.
- Aumann, H. H., S. Broberg, D. Elliott, S. Gaiser, and D. Gregorich (2006a), Three years of Atmospheric Infrared Sounder radiometric calibration validation using sea surface temperatures, *J. Geophys. Res.*, *111*, D16S90, doi:10.1029/2005JD006822.
- Aumann, H. H., D. Gregorich, and S. M. DeSouza-Machado (2006b), AIRS observations of deep convective clouds, paper presented at Photonics Conference, SPIE, San Diego, Calif., 13–17 Aug.
- Chahine, M. T., et al. (2006), The Atmospheric Infrared Sounder (AIRS): Improving weather forecasting and providing new data on greenhouse gases, *Bull. Am. Meteorol. Soc.*, *87*, 911–926.
- Gautier, C., Y. Shiren, and M. D. Hofstadter (2003), AIRS/Vis Near IR Instrument, *IEEE Trans. Geosci. Remote Sens.*, *41*, 330–342.
- Intergovernmental Panel on Climate Change (2001), Model evaluation, in *Climate Change 2001: The Scientific Basis*, edited by J. T. Houghton et al., pp. 471–524, Cambridge Univ. Press, New York.
- Soden, B. J., and R. Fu (1995), A satellite analysis of deep convection, upper-tropospheric humidity, and the greenhouse effect, *J. Clim.*, *8*(10), 2333–2351.
- Strow, L. L., S. E. Hannon, S. De-Souza Machado, H. E. Motteler, and D. C. Tobin (2006), Validation of the Atmospheric Infrared Sounder radiative transfer algorithm, *J. Geophys. Res.*, *111*, D09S06, doi:10.1029/2005JD006146.
- Thiébaux, J., E. Rogers, W. Wang, and B. Katz (2003), A new high-resolution blended real-time global sea surface temperature analysis, *Bull. Am. Meteorol. Soc.*, *84*(5), 645–656.
- Wentz, F. J., and M. Schabel (2000), Precise climate monitoring using complimentary satellite data sets, *Nature*, *403*, 414–416.
- Wentz, F. J., P. D. Ashcroft, and C. L. Gentemann (2001), Post-launch calibration of the TMI microwave radiometer, *IEEE Trans. Geosci. Remote Sens.*, *39*, 415–422.

H. H. Aumann, S. E. Broberg, D. A. Elliott, and D. T. Gregorich, Jet Propulsion Laboratory, California Institute of Technology, 4800 Oak Grove Drive, Pasadena, CA 91109, USA. (aumann@jpl.nasa.gov)